Amorphization of a substitutional binary alloy: a computer 'experiment'

1992 J. Phys.: Condens. Matter 4 2375

(http://iopscience.iop.org/0953-8984/4/10/004)

J. Phys.: Condens. Matter 4 (1992) 2375–2387. Printed in the UK

Amorphization of a substitutional binary alloy: a computer 'experiment'

Lydéric Bocquet, Jean-Pierre Hansen, Thierry Biben and Paul Madden†

Laboratoire de Physique, Unité de Recherche Associée 1325 du CNRS, Ecole Normale Supérieure de Lyon, 69364 Lyon Cédex 07, France

Received 13 December 1991

Abstract. A novel route towards amorphization of an initially crystalline structure is explored by molecular dynamics simulations of a two-dimensional model of 'soft-disk' atoms. Amorphization is driven by a slow increase in the diameters of half the atoms, chosen at random on an initially monodisperse triangular lattice, and a simultaneous reduction in size of the remaining atoms , keeping constant a suitably chosen mean diameter as well as the temperature. The crystal is found to undergo a discontinuous transition towards an amorphous solid at a critical size ratio of the two species. The transition is signalled by jumps of a number of order parameters characterizing the loss of long-range positional and bond-orientational order, and by hysteresis reminiscent of a first-order phase transition. At higher temperatures, a similar adiabatic change in the size ratio leads to melting.

1. Introduction

Many experimental procedures have been devised to generate metastable amorphous structures, starting from one of the thermodynamically stable phases (vapour, melt or crystal) of the same material or its chemical components. One of the most common is based on rapid cooling ('quenching') of the melt. Glasses are routinely obtained by this route from network-forming materials like silica melts. To obtain amorphous metallic compounds from molten alloys, much faster cooling rates have to be applied to bypass crystal nucleation. In the competition between crystallization and glass formation, the latter is favoured by size mismatch of the components, since large differences in atomic sizes are known to drive phase separation on freezing [1, 2]. This requires interdiffusion of the atomic species, which slows down the crystal nucleation rate considerably at low temperatures, particularly under eutectic conditions.

The transition from supercooled liquid to glass in simple models of binary alloys has recently been studied by several groups via molecular dynamics (MD) simulations [3–6]. In these computer 'experiments', the glass was obtained by rapid cooling or compression of the liquid mixture. We propose an alternative numerical *Gedanken-experiment* which leads to an amorphous phase, starting from an initially crystalline solid, made up of a single species of identical atoms.

† Permanent address: Physical Chemistry Laboratory, University of Oxford, South Parks Road, Oxford OX1 3QZ, UK.

0953-8984/92/102375+13$04.50

The key idea is to induce the size asymmetry gradually, by 'swelling' a randomly chosen subset of the originally monodisperse sample, while simultaneously 'shrinking' the remaining atoms, keeping constant a suitably defined mean atomic diameter as well as the total volume of the sample and the temperature. The whole process is carried out sufficiently slowly, so that at each instant the system may be assumed to be in thermodynamic equilibrium, and the transformation may be regarded as reversible. In this way, a substitutionally disordered crystalline alloy is generated continuously, and the reversibility of the path provides a way of computing the free energy of the disordered binary alloy, for each size ratio, by thermodynamic integration [7]. In this paper, we show that, beyond a critical size ratio, the crystalline alloy becomes unstable and undergoes a discontinuous transition to an amorphous binary alloy, signalled by several diagnostics characterizing the loss of long-range order. This irreversible transition between crystalline and amorphous states exhibits hysteresis, as observed in usual first-order phase transitions. The present investigation is restricted to a two-dimensional model, for reasons of simplicity and easier visualization of particle displacements, but we believe that qualitatively similar behaviour would be observed in three dimensions.

2. The model

We consider the two-dimensional, binary 'soft-disk' model, made up of two atomic species, of diameters σ_1 and σ_2, interacting via the purely inverse 12 pair potential,

$$v_{\alpha\beta} = \epsilon(\sigma_{\alpha\beta}/r)^{12} \tag{1}$$

where ϵ defines the energy scale and the diameters are assumed to be additive,

$$\sigma_{\alpha\beta} = \tfrac{1}{2}(\sigma_\alpha + \sigma_\beta) \qquad 1 \leqslant \alpha, \beta \leqslant 2. \tag{2}$$

For a given size ratio, $\lambda = \sigma_1/\sigma_2$ ($\leqslant 1$), the excess equilibrium properties depend only on the concentration, $x_1 = N_1/N$ (where $N = N_1 + N_2$ is the total number of atoms) and on the dimensionless coupling constant,

$$\gamma = \rho^* T^{*-\frac{1}{6}} \tag{3}$$

where $\rho^* = \rho\sigma^2 = N\sigma^2/S$ and $T^* = k_B T/\epsilon$ denote the reduced number density and temperature, and S is the total area of the system; the effective diameter σ will be defined below.

The monodisperse ($\lambda = 1$) soft-sphere fluid undergoes crystallization at $\gamma \simeq 1$, and a reduced pressure $P^* = P\sigma^2/k_B T \simeq 14.5$ [8]. Recent extensive molecular dynamics (MD) simulations have confirmed the first-order nature of the transition [9], rather than a continuous transition involving dislocation unbinding in the crystal and an intermediate hexatic phase [10].

As stated in the introduction, we have carried out extensive MD, as well as Monte Carlo simulations of the binary alloy obtained by gradually decreasing the size ratio from $\lambda = 1$. To that purpose, the diameter σ_2 of half the particles, chosen at random in the original monodisperse crystal, was gradually increased above the initial common value σ, while at the same time the diameter σ_1 of the remaining N/2 atoms was

reduced; all simulations were thus made for an equimolar alloy ($x_1 = x_2 = 1/2$). The simultaneous particle 'swelling' and 'shrinking' was carried out in such a way that the effective diameter, appropriate for a one component ('conformal solution') description of the binary mixture was held fixed, and equal to the initial monodisperse value σ. Within conformal solution theory [11], the resulting constraint on the diameters of the two species reads:

$$x_1^2\sigma_{11}^2 + 2x_1x_2\sigma_{12}^2 + x_2^2\sigma_{22}^2 = \sigma^2 \tag{4}$$

which uniquely determines σ_1 and σ_2 for any choice of the size ratio $\lambda = \sigma_1/\sigma_2$. For a given initial value σ, the pair potential (1) may now be regarded as a continuous function of λ, $v_{\alpha\beta}^{\lambda}(r)$. Similarly, for fixed temperature T, area S and concentration x_1, the partition function is also a continuous function of the size ratio, i.e. $Q_N(\lambda)$. The excess free energy of the mixture (or alloy) is then related to that of the initial monodisperse system by straightforward integration [7, 11, 12],

$$F_{ex}(\lambda) = F_{ex}^0 + \int_1^{\lambda} \left\langle \frac{\partial V_N^{\lambda'}}{\partial \lambda'} \right\rangle_{\lambda'} d\lambda' \tag{5}$$

where $F_{ex}^0 = F_{ex}(\lambda = 1)$ is the free energy of the monodisperse 'reference system', and $V_N^{\lambda'}$ denotes the total potential energy of the mixture for a given value of the size ratio:

$$V_N^{\lambda} = \frac{1}{2}\sum_{\alpha}\sum_{\beta}\sum_{i\neq j} v_{\alpha\beta}^{\lambda}(r_{ij}). \tag{6}$$

The sum in (6) is taken over all particles species ($1 \leqslant \alpha, \beta \leqslant 2$) and over all pairs of atoms (i, j) in the mixture, at mutual distances r_{ij}. The statistical average in the integrand of (5) is taken over an ensemble of mixtures with potential energy V_N^{λ}. Equation (5) will yield the free energy of the mixture as long as the path parametrized by λ is reversible. Note that, for convenience, the masses of the two species are held constant during the transformation.

The natural time unit in the MD simulations is $\tau = (\epsilon/ma^2)^{1/2}$, where m is the particle mass, while $a = (\pi\rho)^{-1/2}$ is the radius of a disk containing on average one atom. All simulations were carried out for a fixed value of the density, while the temperature was held constant by the use of a Hoover thermostat [13]; consequently, all results reported below correspond to fixed values of γ. The gradual reduction of the size ratio λ was implemented very gently by a succession of small jumps, $\Delta\lambda \simeq 10^{-5}$, separated by re-equilibration periods lasting 10^2 time steps (of length $\Delta t \simeq 5.10^{-3}\tau$) during which λ was held constant. Thus, in a typical run lasting 10^4 time steps, λ was reduced by a few parts in a thousand; each 'reduction' run was followed by a 'production' run , during which λ was held constant, and statistical averages were taken over at least 10^4 time steps. All simulations reported here were made for samples of $N=108$ atoms in a hexagonal cell, with periodic boundary conditions. A cross-check of the data reported below was provided by a number of MC simulations which we performed for identical thermodynamic states and size ratios. Two series of simulations were carried out; the first series was for $\gamma = 1.64$, well inside the crystal phase of the monodisperse system, while the second was for $\gamma = 1.05$, close to the melting point of the monodisperse crystal.

3. Diagnostics

At the monodisperse starting points ($\lambda = 1$), the soft-disk system forms a triangular crystal, since λ was chosen to be larger than its value at freezing ($\lambda \simeq 1$). However, the binary crystalline alloy is expected to become unstable beyond a critical size asymmetry. In order to characterize the expected loss of long-range order, we monitored a certain number of 'diagnostics' while λ was gradually reduced.

To estimate the degree of translational order, we calculated the mean value of the modulus of:

$$\rho_G = \frac{1}{N}\sum_{i=1}^{N} \exp\{\mathrm{i}\boldsymbol{G}\cdot\boldsymbol{r}_i\} \tag{7}$$

where $\boldsymbol{r}_i$ denotes the instantaneous position of atom i, while $\boldsymbol{G}$ is a reciprocal lattice vector. $\langle|\rho_G|\rangle = 1$ for a perfect crystal, where each atom occupies a lattice site, whereas this average is expected to be of the order of $1/\sqrt{N}$ for a completely disordered structure. Another measure of the loss of crystalline order is provided by

$$\langle\Delta r\rangle^2 = \frac{1}{N}\sum_{i=1}^{N}(\langle r_i\rangle - r_{i0})^2 \tag{8}$$

where r_{i0} is the triangular lattice position of the ith atom. This quantity, which vanishes identically for a perfect crystal, should not be confused with the vibrational mean-square displacement,

$$\langle|u|^2\rangle = \frac{1}{N}\sum_{i=1}^{N}\langle(r_i - \langle r_i\rangle)^2\rangle \tag{9}$$

Positional correlations are measured by computing the usual pair-distribution function $g(r)$ defined by [11]:

$$\rho g(r) = \frac{1}{N}\int\langle\hat{\rho}(r')\hat{\rho}(r'+r)\rangle\mathrm{d}r' - \delta(r) \tag{10}$$

where $\rho(r')$ denotes the microscopic density,

$$\rho(r') = \sum_{i=1}^{N}\delta(r' - r_i). \tag{11}$$

In the (presumably) isotropic amorphous phase, $g(r)$ depends only on the relative distance $r = |r|$, while in the crystalline solid, $g(r)$ was averaged over orientations of r.

Bond-orientational order is conveniently characterized by the Nelson–Halperin order parameter [10],

$$\langle\Psi\rangle = \frac{1}{N}\sum_{i=1}^{N}\langle\Psi_i\rangle = \frac{1}{N}\sum_{i=1}^{N}\left\langle\frac{1}{n_i}\sum_{j=1}^{n_i}\mathrm{e}^{\mathrm{i}6\theta_{ij}}\right\rangle. \tag{12}$$

On the right-hand side of (12), θ_{ij} is the bond angle of an (i,j) pair of nearest neighbours relative to a fixed polar axis, while the sum over j is taken over all n_i nearest neighbours of particle i. Again $\langle\Psi\rangle$ takes on the value 1 for a perfect triangular crystal, while it vanishes in a locally disordered structure. In the same spirit, we also calculated the fraction of atoms having exactly six nearest neighbours as determined by a Voronoï polygon construction,

$$f_6 = \frac{1}{N}\left\langle \sum_{i=1}^{N} \delta_{n_i,6} \right\rangle. \tag{13}$$

The correlation of local bond-orientational order may be measured from the function:

$$G_6(r) = \frac{\frac{1}{N}\int\langle\hat{\Psi}(r')\hat{\Psi}(r'+r)\rangle \mathrm{d}r'}{\frac{1}{N}\int\langle\hat{\rho}(r')\hat{\rho}(r'+r)\rangle \mathrm{d}r'} \tag{14}$$

where the local 'orientational density' is defined by:

$$\hat{\Psi}(r') = \sum_{i=1}^{N} \delta(r' - r_i)\Psi_i. \tag{15}$$

4. The transition

Proceeding as described in section 2, we computed the various order parameters and correlations functions introduced in section 3 as functions of the size ratio λ, for $\gamma = 1.64$ and $\gamma = 1.05$. The MD results for the translational- and orientational-order parameters $\langle\Delta r\rangle^2$, $\langle|\rho_{G_1}|\rangle$ (where G_1 is the smallest reciprocal lattice vector), $\langle\Psi\rangle$ and f_6 are plotted against λ in figure 1(*a*) for $\gamma = 1.64$. The four order parameters are seen to decrease (increase in the case of $\langle\Delta r\rangle^2$) only slightly as the size ratio is reduced from $\lambda = 1$ to $\lambda \simeq 0.78$. At that stage, all four order parameters undergo a sharp discontinuity signalling the loss of long-range translational and bond-orientational order. The crucial observation is that the four discontinuities occur at exactly the same value of the size ratio. Their location is moreover perfectly reproducible as shown in figure 1(*b*) from the data obtained for a different sample, corresponding to a different random choice on the initial monodisperse lattice of the 54 atoms to be 'swollen' or 'shrunk'. While the discontinuities occur at exactly the same value of λ as in figure 1(*a*), the amplitudes of the jumps are somewhat different, particularly so for the translational-order parameters. We attribute these differences to the lack of sufficient self-averaging in the 108-particle samples used in our simulations.

The loss of the initial crystalline order is due to fairly small local rearrangements of the equilibrium positions $\langle r_i\rangle$ of the N atoms, as illustrated in figure 2. Once the atoms have found new equilibrium positions differing from the initial triangular lattice sites, they vibrate around these positions, but remain localized, contrary to the case of a liquid, where they would undergo diffusion. This behaviour is typical of an amorphous solid, and explains why the order parameters $\langle|\rho_{G_1}|\rangle$ and $\langle\Psi\rangle$ remain non-zero after the transition in a small system, contrary to the case of two-dimensional

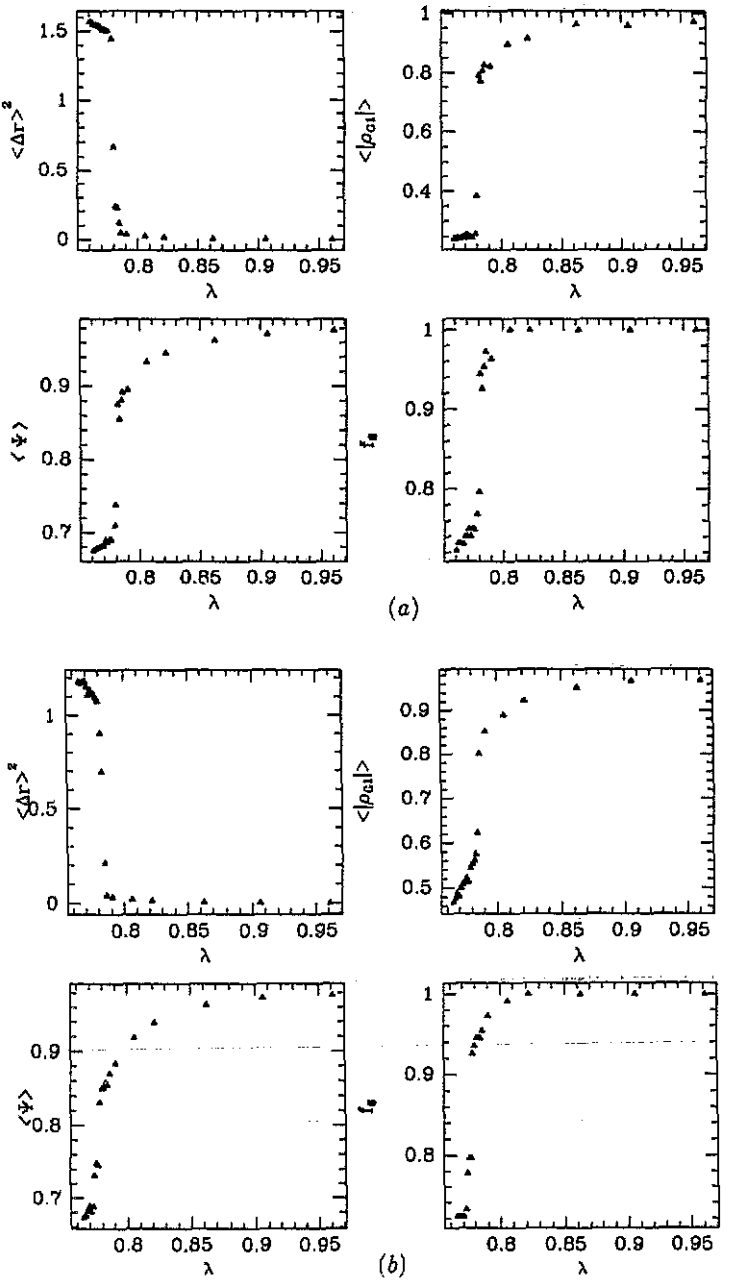

Figure 1. (*a*) Variation of the order parameters $\langle \Delta r \rangle^2$ (8) $\langle |\rho_{G_1}| \rangle$ (7) $\langle \Psi \rangle$ (12) and f_6 (16) with the size ratio $\lambda = \sigma_1/\sigma_2$, starting from the monodisperse crystal ($\lambda = 1$) at $\gamma = 1.64$. (*b*) Same as (*a*), but for a different random initial assignment of 'growing' and 'shrinking' atoms.

melting, which atomic diffusion allows an efficient sampling of phase space. The sharpness of the transition is also illustrated by the considerable difference in the correlation functions $g(r)$ and $G_6(r)$ just before ($\lambda = 0.781$) and after ($\lambda = 0.779$)

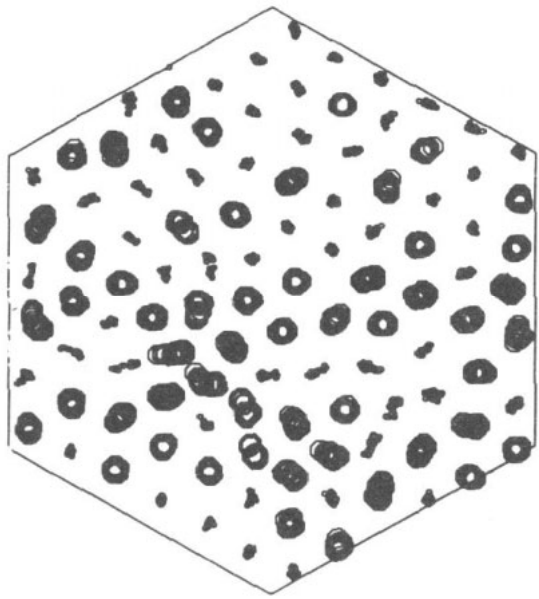

Figure 2. Evolution of the equilibrium position of the 108 atoms with time, for $\gamma = 1.64$, $\lambda = 0.779$. The starting point is the final configuration obtained in the crystal phase at $\lambda = 0.781$. The positions of the large (small) atoms are represented by large (small) polygons.

the transition, as shown in figures 3 and 4. In particular, the envelope of the bond-orientational correlation function $G_6(r)$, which is still nearly constant at $\lambda = 0.781$ decreases smoothly for $\lambda \leqslant 0.779$; moreover it turns out to change very little with λ, for $\lambda \leqslant 0.778$.

It is tempting to interpret the discontinuities of the order parameters and correlation functions as the limit of metastability associated with a first-order phase transition between the substitutionally disordered crystal and the amorphous alloy. This interpretation is strengthened by the hysteresis which is clearly apparent upon reversing the process, by increasing the size ratio λ, starting from an initial amorphous state obtained for $\lambda < 0.78$. The hysteresis is illustrated in figure 5 for the order parameters $\langle|\rho_{\mathbf{G}1}|\rangle$ and $\langle\Psi\rangle$. On slowly decreasing λ from the crystal side, the discontinuities are observed to occur at $\lambda \simeq 0.780$, while on a gradually increasing λ starting from the amorphous solid, the jumps occur when the size ratio goes through the value $\lambda \simeq 0.805$, after which the order parameters retrace their values in the crystal phase; similar hysteresis is observed for the other order parameters.

With the objective of seeking a thermodynamic characterization of the transition, we computed the equation of state, $\beta P/\rho$, from the virial theorem, and the integrand $J(\lambda) = \langle \partial \beta V_N^\lambda / \partial \lambda \rangle_\lambda / N$ of the free energy (5), as functions of λ. Both quantities exhibit discontinuities and hysteresis, shown in figures 6 and 7(*a*), which closely parallel the behaviour of the order parameters. The absolute Helmholtz free energy was calculated for the monodisperse crystal ($\lambda = 1$) and for the bi-disperse amorphous solid ($\lambda = 0.76$), by the method of Frenkel and Ladd [14]. Free energies for other values of λ were obtained in both phases by integration of $J(\lambda)$, according to (5); the results are plotted in figure 7(*b*), together with the estimates obtained within the harmonic phonon approximation (see the appendix for details). The two free energy

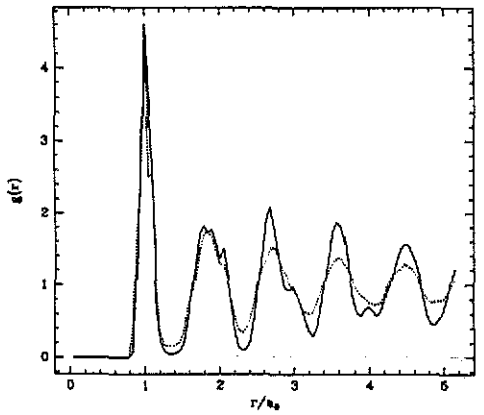

Figure 3. Mean pair-distribution functions computed for $\gamma = 1.64$ in the crystal phase, at $\lambda = 0.781$ (full curve) and in the amorphous phase at $\lambda = 0.779$ (dashed curve). The distance r is measured in units of the triangular lattice spacing a_0; the $g(r)$ are averaged over the three types of pairs (1–1,1–2 and 2–2).

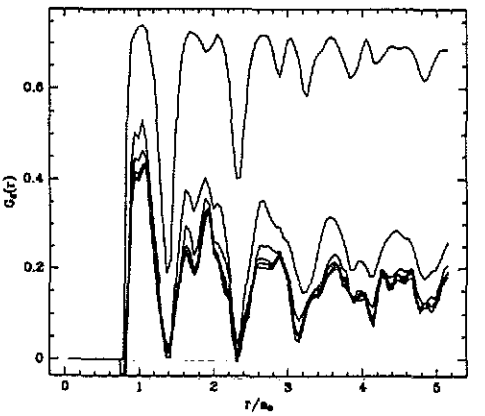

Figure 4. Bond-orientational correlation function $G_6(r)$ (14) against r/a_0 for $\gamma = 1.64$ and $\lambda = 0.781$ (crystal phase, upper curve), $\lambda = 0.779, 0.778, 0.777, 0.775, 0.774$ and 0.772 (amorphous phase). Note that the curves for the last five size ratios, λ, practically coincide.

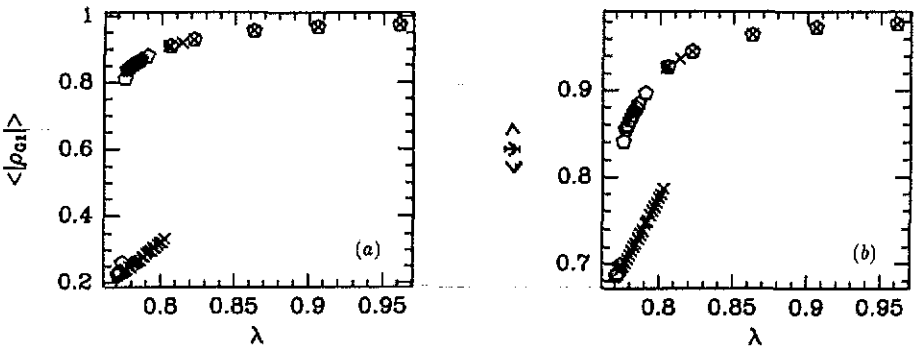

Figure 5. Hysteresis of the order parameters, (*a*) $\langle|\rho_{G_1}|\rangle$ and (*b*) $\langle\Psi\rangle$, at $\gamma = 1.64$. The pentagons are the MD data collected on decreasing the size ratio from the monodisperse crystal ($\lambda = 1$), while the crosses are the results obtained on increasing λ, starting from the amorphous solid.

curves are found to intersect at $\lambda \simeq 0.79$, roughly half-way between the two limits of metastability, as one would expect for a first-order phase transition. According to the results shown in figure 5, the pressures of the two phases are equal for that size ratio, within statistical uncertainties. Since, for the potentials (1), the reduced excess internal energy per particle is related to the equation of state by:

$$u = \beta U^{ex}/N = \tfrac{1}{6}[(\beta P/\rho) - 1] \tag{16}$$

we conclude that the entropies of the two phases must be practically equal (with

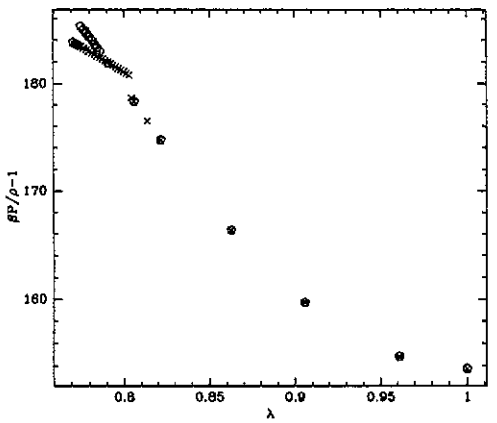

Figure 6. Equation of state, $\beta P/\rho$ against size ratio λ for $\gamma = 1.64$. The pentagons and crosses have the same meaning as in figure 5 (hysteresis).

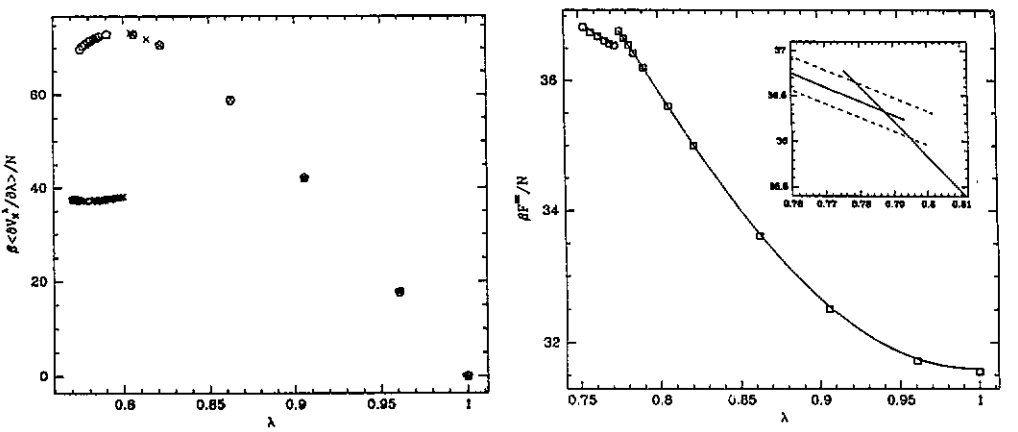

Figure 7. (*a*) $J(\lambda) = \beta\langle\partial V_N^\lambda/\partial\lambda\rangle_\lambda$ against λ for $\gamma = 1.64$. Pentagons and crosses have the same meaning as in figure 5 (hysteresis). (*b*) Excess free energy per particle, $\beta F^{ex}/N$, obtained by integrating $J(\lambda)$ shown in figure 7(*a*) (full curve). The estimates based on harmonic phonon theory are shown as squares. The insert shows a blow-up of the region where free energies of the crystal and of the amorphous solid intersect. The dashed curves parallel to the amorphous solid branch represent the statistical uncertainties of the free energy in that phase.

an estimated uncertainty $\Delta S/Nk_B = (\Delta U - \Delta F)/Nk_BT \leqslant 0.1$) at the transition point $\lambda \simeq 0.79$.

The size ratio, λ, plays the role of an additional intensive thermodynamic variable and the differential of the free energy reads:

$$dF = -S\,dT - P\,dV + \sum_\alpha \mu_\alpha\,dN_\alpha + Nk_BTJ\,d\lambda. \tag{17}$$

Now thermodynamic stability requires that the second derivatives of F with respect to intensive variables (T and λ in the present case) are negative. This implies that

$$(\partial J/\partial\lambda)_{T,V,\{N_\alpha\}} < 0. \tag{18}$$

This is precisely the behaviour shown in figure 7(*a*): the system is found to 'jump' from one phase to the other shortly after the slope of the J–λ curve changes sign,

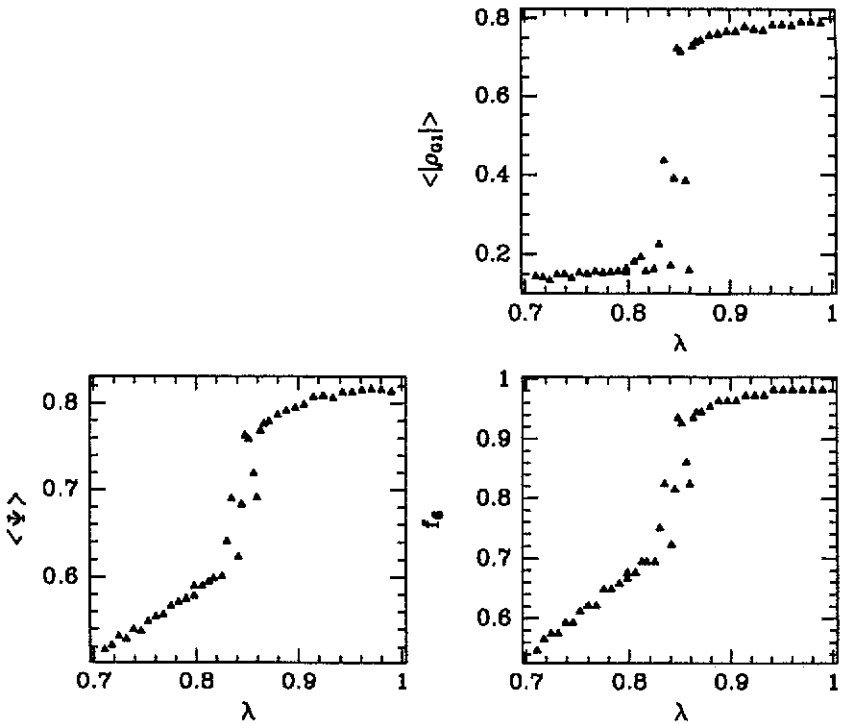

Figure 8. Order parameters $\langle|\rho_{G_1}|\rangle$, $\langle\Psi\rangle$ and f_6 against size ratio λ for $\gamma = 1.05$.

both on decreasing and increasing the size ratio. The lack of strict correspondence between the change in sign and the jump must be attributed to finite size effects.

We carried out a second set of simulations for a value of the coupling parameter, $\gamma = 1.05$, much closer to its value at the melting point of the monodisperse ($\lambda = 1$) system. Since on decreasing the size ratio, λ, a eutectic point should occur in the fluid–solid phase diagram [2], whereby freezing must take place at a higher value of γ, it is reasonable to expect that the crystal will melt spontaneously below some critical λ. This is indeed the behaviour observed from the MD data around $\lambda = 0.85$. However, as shown from the variation of the order parameters in figure 8, the transition is less sharp than at $\gamma = 1.64$, since the jumps appear to be 'smeared' over a certain range of size ratios. The apparent width of the transition may be traced back to oscillations of the system back and forth between a crystalline and a fluid state, contrary to the irreversible jump from crystal to amorphous solid observed at $\gamma = 1.64$. This interpretation is confirmed by inspection of instantaneous configurations, which exhibit fractions of six-fold coordination, f_6, fluctuating between 1 (perfect crystal) and 0.6 (with equal numbers of five-fold and seven-fold coordinated atoms, corresponding to as many dislocations). The two types of configurations nicely correlate with the bimodal distribution of internal energies shown in figure 9. The identification of the disordered phase as a fluid phase is justified by the observation that the atoms diffuse away from their initial positions, following the usual Einstein relation $\langle|r(t) - r(0)|^2\rangle \sim t$. All our observations are compatible with the interpretation that the states ($\gamma = 1.05; 0.8 \leqslant \lambda \leqslant 0.86$) fall into the two-phase region; as usual for small systems, coexistence of the fluid and solid phases is not possible due to the relative importance of interfacial effects, forcing the system to make frequent

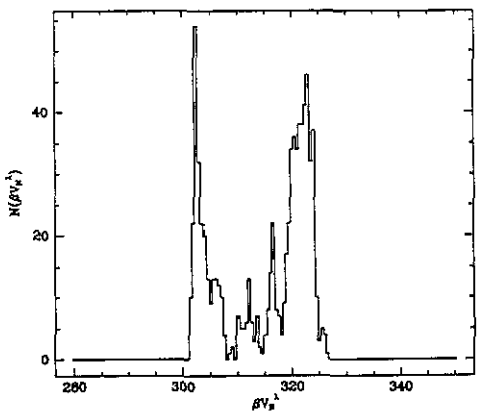

Figure 9. Distribution of excess internal energies, $N(\beta V_N^{\lambda})$, observed during the MD run at $\gamma = 1.05$, $\lambda = 0.834$.

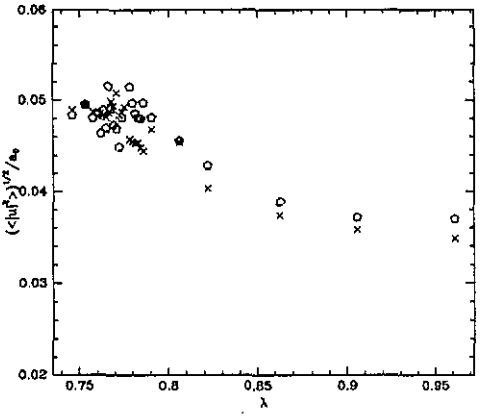

Figure 10. Root-mean-square displacement $((|\boldsymbol{u}|^2))^{1/2}$ against size ratio λ for $\gamma = 1.64$. The pentagons are the MD data, while the crosses correspond to the harmonic phonon analysis, using the equilibrium positions $\boldsymbol{R}_i$ of the atoms taken from the MD runs.

jumps between the two (metastable) bulk phases. It should be stressed that, according to the results of [2], the bi-disperse crystalline alloy is probably metastable and that the state of lowest free energy involves coexistence of two crystal phases of different compositions with the melt. Due to the extremely slow interdiffusion process, this state of lowest free energy is far outside the reach of the time scales covered by the simulations.

5. Discussion

On the basis of extensive MD simulations, we have shown that a discontinuous transition, from a two-dimensional hexagonal crystal to an amorphous solid, may be induced by a quasi-static variation in the ratio of the atomic diameters in a random alloy. The discontinuous jump from the ordered to the disordered structure exhibits all the characteristic features of a first-order thermodynamic phase transition, including hysteresis. The observed order–disorder transition cannot, however, be considered as a genuine equilibrium phase transition, since the bi-disperse crystal and amorphous solid are almost certainly metastable with respect to a pair of coexisting crystal phases having different chemical compositions. The transition towards the state of lowest free energy, which would involve an extremely slow interdiffusion process in the original random alloy, is preempted by the amorphization observed in our simulations, involving only modest local rearrangements of atomic positions which destroy long range translational and bond-orientational order. The transition between the crystalline and amorphous alloys behaves quite differently from the melting transition observed at higher temperatures, which involves coexistence of the ordered crystal and the disordered fluid, as signalled by frequent jumps between both phases in the small sample simulated in the present work.

Despite the fact that the present transition is not a proper equilibrium phase transition, it is interesting to note that it does not depend on the mass ratio of the two species. Indeed, Monte Carlo simulations carried out in parallel, which explore configuration (rather than phase) space, and are hence independent of particle masses, yield order parameters, static correlation functions and thermodynamic properties that are identical, within statistical errors, to those obtained by MD simulations which map out trajectories in phase space, depending explicitly on the masses.

The extension of the present simulations to three-dimensional bi-disperse solids should be straightforward and we expect that a qualitatively similar order–disorder transition would be observed upon varying the size ratio. The obvious question is whether the transition, driven by a change in atomic characteristics and hence of the system's Hamiltonian, is only observable in numerical 'experiments' or whether it has a physical counterpart in the laboratory. A possible laboratory experiment would be to compress a crystalline substitutional binary alloy containing one species which undergoes an electronic transition and hence 'shrinks' under pressure (like Cs), and another atomic species which is essentially incompressible. The 'collapse' of the first species could then lead to an amorphization similar to the one reported here.

Acknowledgments

One of us (JPH) acknowledges a fruitful conversation with Pierre Aigrain. Part of this work was carried out while Paul Madden held the Louis Néel Chair of the Ecole Normale Supérieure de Lyon, sponsored by the Société Lyonnaise de Banque.

Appendix

We made systematic comparisons between the MD data and a harmonic phonon analysis of the crystalline and amorphous solid. Following the standard procedure, the total potential energy (6) is expanded to second order in the displacements $\boldsymbol{u}_i = \boldsymbol{r}_i - \boldsymbol{R}_i$ from their equilibrium positions $\boldsymbol{R}_i = \langle \boldsymbol{r}_i \rangle$. In the disordered solid, the latter, which are frozen, are taken from the MD averages and serve only as input to the harmonic calculation. Dropping the subscript λ in equation (6), V_N may be cast in the harmonic form,

$$V_N(\boldsymbol{r}_1 \ldots \boldsymbol{r}_N) = V_N(\boldsymbol{R}_1 \ldots \boldsymbol{R}_N) + \tfrac{1}{2} u_i^\mu D_{ij}^{\mu\nu} u_j^\nu \tag{A1}$$

where summation is understood over repeated particle (i, j) and Cartesian (μ, ν) indices. $D_{ij}^{\mu\nu}$ is the real-space dynamical matrix,

$$\begin{aligned} D_{ij}^{\mu\nu} = & \delta_{ij} \sum_{k \neq i} [\alpha_{ik} \delta_{\mu\nu} + (\beta_{ik} - \alpha_{ik}) n_{ik}^\mu n_{ik}^\nu] \\ & - (1 - \delta_{ij}) [\alpha_{ij} \delta_{\mu\nu} + (\beta_{ij} - \alpha_{ij}) n_{ij}^\mu n_{ij}^\nu] \end{aligned} \tag{A2}$$

where n_{ij}^μ are the Cartesian components of the unit vector $\boldsymbol{r}_{ij}/|\boldsymbol{r}_{ij}|$, while

$$\alpha_{ij} = \frac{v_{ij}'(|\boldsymbol{R}_i - \boldsymbol{R}_j|)}{|\boldsymbol{R}_i - \boldsymbol{R}_j|} \tag{A3a}$$

$$\beta_{ij} = v_{ij}''(|\boldsymbol{R}_i - \boldsymbol{R}_j|). \tag{A3b}$$

The N coupled, harmonic equations of motion then read:

$$m_i \ddot{u}_{i\mu} = -D_{ij}^{\mu\nu} u_{j\nu} \tag{A4}$$

where dots stand for time derivatives. As usual, periodic solutions are sought; the squares of the $2(N\text{-}1)$ harmonic angular frequencies, ω_n, are eigenvalues of the dynamical matrix $D_{ij}^{\mu\nu}/m$. The $2(N\text{-}1)$ (214 in the present case) ω_n were calculated by numerical diagonalization of the dynamical matrix.

The eigenfrequencies ω_n were used to calculate the classical harmonic free energy,

$$\frac{\beta F_{\text{harm}}}{N} = \frac{\beta V(\boldsymbol{R}_1, \ldots, \boldsymbol{R}_N)}{N} + \sum_n \log\left(\frac{\hbar\omega_n}{k_B T}\right) \tag{A6}$$

shown in figure 7(*b*), and the mean square displacement (averaged over all particles),

$$\langle |\boldsymbol{u}|^2 \rangle = \frac{1}{N-1} \sum_n \frac{k_B T}{m\omega_n^2}. \tag{A7}$$

The harmonic approximation slightly underestimates the mean square displacement, which is seen to increase with decreasing size ratio (figure 10). The data become very noisy in the transition region, but they seem to be compatible with a levelling off, or even a small drop of $\langle |\boldsymbol{u}|^2 \rangle$, which would lead to a lowering of the vibrational entropy in the amorphous solid, compared to the crystal. Note that the errors affecting the harmonic values of $\langle |\boldsymbol{u}|^2 \rangle$ in the amorphous solid reflect the uncertainties of the MD estimates of the equilibrium position $\boldsymbol{R}_i$.

References

[1] Hume-Rothery W, Smallman E R and Haworth C W 1969 *The Structure of Metals and Alloys* (London: The Metals and Metallurgy Trust)

[2] Barrat J L, Baus M and Hansen J P 1986 *Phys. Rev. Lett.* **56** 1063
Xu H and Baus M 1990 *J. Phys.: Condens. Matter* **2** 5885

[3] Bernu B, Hansen J P, Hiwatari Y and Pastore G 1987 *Phys. Rev.* A **36** 4891

[4] Mountain R D and Thirumalai D 1987 *Phys. Rev.* A **36** 3300

[5] Jonsson H and Andersen H C 1988 *Phys. Rev. Lett.* **60** 2295

[6] Barrat J L, Roux J N and Hansen J P 1990 *Chem. Phys.* **149** 197

[7] Kranendonk W G T and Frenkel D 1991 *Mol. Phys.* **72** 699

[8] Broughton J Q, Gilmer G H and Weeks J D 1982 *Phys. Rev.* B **25** 4651

[9] Andersen H C 1991 private communication

[10] Nelson D R and Halperin B I 1980 *Phys. Rev.* B **21** 5312

[11] See for example Hansen J P and McDonald I R 1986 *Theory of Simple Liquids* 2nd edn (London: Academic Press)

[12] Singer J V L and Singer K 1972 *Mol. Phys.* **24** 357

[13] Hoover W G 1985 *Phys. Rev.* A **31** 308

[14] Frenkel D and Ladd A J C 1984 *J. Chem. Phys.* **81** 3188